Journal of Applied Polymer Science

Synthesis and Properties of a Superabsorbent from an Ultraviolet-Irradiated Waste Nameko Mushroom Substrate and Poly(acrylic acid)

Mingyue Zhang,[1] Zhiqiang Cheng,[1,2] Mengzhu Liu,[1] Yongqiang Zhang,[1] Meijuan Hu,[1] Junfeng Li[1]

[1]College of Chemistry, Jilin University, Changchun 130012, People's Republic of China

[2]College of Resources and Environment, Jilin Agriculture University, Changchun 130118, People's Republic of China

Correspondence to: J. Li (E-mail: jfli@jlu.edu.cn)

ABSTRACT: To better use the waste nameko mushroom substrate (WNMS) and prevent its pollution into the environment, a novel superabsorbent polymer was synthesized via the UV irradiation copolymerization of acrylic acid and WNMS in the presence of an initiator (dimethoxy-2-phenylacetophenone and ammonium persulfate) and crosslinker *N,N′*-methylenebisacrylamide. The factors that had an influence on the water absorbency of the superabsorbent polymer were investigated and optimized. Under the optimized conditions, WNMS–poly(acrylic acid) was obtained. Its swelling behaviors, which followed the pseudo-second-order swelling kinetic model, were investigated in distilled water (1701 g/g) and a 0.9 wt % NaCl solution (388 g/g). The water absorbency was 1011 g/g in a 0.1 wt % urea solution and 80% amount of urea diffused into the gels. The urea diffusion followed a Fickian diffusion mechanism. Moreover, the product showed excellent water retention capabilities under the condition of high temperature or high pressure. © 2014 Wiley Periodicals, Inc. J. Appl. Polym. Sci. **2014**, *131*, 40471.

KEYWORDS: adsorption; crosslinking; gels; hydrophilic polymers; swelling

Received 14 November 2013; accepted 17 January 2014

DOI: 10.1002/app.40471

INTRODUCTION

Superabsorbent hydrogels are three-dimensional crosslinked hydrophilic polymers with the ability to absorb larger quantities of pure water or aqueous solutions compared to traditional absorbent materials, such as sponges, cotton, and pulp.[1] The superabsorbent hydrogels not only have a high water absorbency but also exhibit an excellent water retention (WR) capacity. In addition, the hydrogels display a slower water-releasing rate than traditional materials even under the same conditions.[2,3] Because of these superior performances, superabsorbent polymers are widely used in many specialized applications, such as drug-delivery systems,[4,5] coal dewatering, hygienic products,[5] wastewater treatment,[6] metal-ion removal,[7] horticulture, and agriculture.[8,9]

Recently, many superabsorbent polymers have been synthesized with polysaccharide-based natural materials;[10–15] this could increase their biocompatibility, biodegradability, and water absorbent capacity and decrease their toxicity. Among these natural materials, cellulose has been studied extensively because of its abundant reserves. However, the effective use of existing resources is significant in contemporary society. Thus, it is quite necessary to study the reuse of waste materials. In the world, millions of tons of mushrooms are produced per year. As a byproduct of mushroom cultivation, waste nameko mushroom substrate (WNMS; the mushroom cultivation substrates consist of corn cobs and sawdust, and it can be obtained after the growth of nameko mushrooms), which primarily consists of natural cellulose and hemicelluloses (10–30%), protein (6–13%), and crude fat (1–5%),[16,17] is an abundant bioresource. Unfortunately, only a small portion of WNMS is used in organic fertilizers and flower soils. Most WNMS is discarded or burned; this leads to the waste of resources and environmental pollution. In view of this situation, we considered WNMS for use as a raw material in the synthesis of superabsorbent hydrogels. Thus, the disadvantages mentioned previously could be prevented, and most of all, the reuse of waste substrate could be accomplished.

Conventional synthetic methods for producing superabsorbent polymers are time-consuming and often require expensive specialized equipment to maintain the necessary reaction conditions. Recently, new synthesis technologies, such as microwave irradiation,[18,19] ultrasound,[20] γ irradiation,[21] and UV irradiation,[19,22] have been developed. Among those methods, UV irradiation can shorten the reaction time[23] and improve the efficiency.[24,25] The environmental impact of irradiation technology is also more manageable and applicable as a dry reaction or semidry reaction processes.

© 2014 Wiley Periodicals, Inc.

In this study, a novel superabsorbent polymer WNMS–poly(acrylic acid) (PAA) was synthesized by UV irradiation. The introduction of WNMS–PAA was expected to provide a new way to extend the utilization of WNMS, what is more, to lower the cost of production and improve the biocompatibility and biodegradability of the superabsorbent. WNMS–PAA can be used in agriculture to retain water and as a fertilizer. The effects of the preparation conditions, such as the contents of crosslinker, initiators, and WNMS; reaction time; and acrylic acid (AA) neutralization degree, on the water absorption abilities in distilled water and 0.9 wt % NaCl solutions were discussed. This polymer was characterized by Fourier transform infrared (FTIR) spectroscopy, scanning electron microscopy (SEM), and thermogravimetry (TG)/derivative TG. Furthermore, the swelling kinetics and urea diffusion mechanism were systematically investigated.

EXPERIMENTAL

Materials and Methods

Materials. AA (analytically pure, Tianjin Fuchen Chemical Reagent Co., Ltd., China) was purified under reduced pressure. Ammonium persulfate (APS; analytically pure) was from Tianjin Fuchen Chemical Reagent Co., Ltd. (China). *N,N′*-Methylenebisacrylamide (MBA; purity > 99.9%), dimethoxy-2-phenylacetophenone (BDK), methanol, sodium hydroxide, and sodium chloride were from Beijing Chemical Works (Beijing, China). Urea (Xilong Chemical Co., Ltd., Guangdong China), paradimethyl aminobenzaldehyde (Tianjin Guangfu Fine Chemical Institute, Tianjin, China), and all of the other reagents were all of analytical grade and were used directly as purchased. WNMS (particle size = 120 mesh) was acquired from the Bacteria Institute of Jilin Agricultural University (Jilin, China) and used without further purification.

Preparation of the WNMS–PAA, PAA Superabsorbent Composite. The required amount of AA was added to a certain amount of a 20 wt % NaOH solution in a 500-mL glass beaker, which was placed in an ice bath with constant stirring, to obtain a series of different neutralization degrees of AA solution. The prepared solutions were mixed with different quantities of WNMS, MBA (0.02 g/mL), APS, and BDK (0.05 g/mL) in 50-mL glass beakers and were subjected to ultrasound pretreatment in an air atmosphere for 1 min. The specific parameters of each experiment are shown in Table I. The effects of the variable conditions, such as the reaction time, neutralization degree of AA, and crosslinker and initiator contents, on the swelling behavior were examined. When one factor was studied, the other variable conditions were kept constant. Then, homogeneous mixtures were exposed to a UV lamp for several minutes [the self-regulated UV irradiation system consisted of an iron box containing an UV lamp (1000 W) with a wavelength of 365 nm.]. The distance between the reaction mixture and the light source was 37 cm. Thereafter, the gels obtained were immersed in a methanol solution to remove the water-soluble oligomer, uncrosslinked polymer, and unreacted monomer. Finally, the gel was dried in a vacuum oven at 70°C to a constant weight and crushed into 150–300-μm particles for use. WNMS–PAA represented the polymer obtained under the optimal conditions which had the largest water absorbency. PAA was synthesized according to the previous method, and the mass ratios of AA to WNMS to MBA to APS to BDK was 100:0: 0.12:0.40:0.25. The neutralization degree of AA was 85%, and the reaction time was 20 min. The proposed mechanism of hydrogel formation is shown in Figure 1. First, the BDK initiator and $(NH_4)_2S_2O_8$ initiator decomposed into benzoyl and sulfate radicals under UV irradiation. Second, these radicals reacted with the cellulose chain in WNMS. Then, the ring structure of β-D-glucose in cellulose was broken, and this resulted in the formation of some more active groups, such as alkoxy radicals. The AA monomer molecule reacted with these groups, and this led to the growth of polymer chain. Finally, the polymer chains reacted with the end vinyl groups of the crosslinker (MBA) during chain propagation. As a result, the crosslinked structure combined with the network structure was formed gradually.[14]

Water Absorbency Measurement. The water absorbency of the hydrogel (Q_t; g/g) was examined by the immersion of approximately 0.10 g of hydrogel in 500 mL of distilled water at room temperature (25°C) at different intervals [time (t; min)] until swelling equilibrium (360 min) was reached.[26] The swollen sample was filtered through a 100-mesh nylon bag to separate unabsorbed water and was then weighed. The swelling capacity of the polymer was calculated by the following equation:

$$Q_t = \frac{m_t - m_0}{m_0} \quad (1)$$

where m_0 and m_t are the weights of the dry and wet samples at a specified time (g), respectively. The water absorbency in the 0.9 wt % NaCl solution and 0.1 wt % urea solution were tested in the same way.

Swelling and Urea Diffusion Characteristics in a Urea Solution. To study the swelling of the hydrogel and urea diffusion in a 0.1 wt % urea solution, approximately 0.10 g of the WNMS–PAA polymer was placed in 500 mL of urea solution (0.1 wt %) under stirring conditions at room temperature (25°C). Then, the gel and unabsorbed urea solution were separated at different times. The urea content contained in the solution before and after the addition of hydrogel was determined with ultraviolet–visible spectrophotometry at 430 nm.[27] Then, the amount of urea diffused into the gel at time t (M_t) was obtained. All of the experiments of urea content were performed in triplicate, and the results were averaged.

Determination of Water Retention. The percentage WR was determined by the weights of the water-swollen gel before centrifugation (M_1; g) and after centrifugation (M_2; g) at 6000 rpm ($M_1 \approx 40$ g, centrifugal radius = 8.6 cm) at set intervals (0, 5, 10, 15, 20, 25, 30, 35, 40, 45, 50, and 60 min) or heating at 60°C ($M_1 \approx 75$ g) in an air oven at set intervals (0, 100, 200, 300, 400, 500, 600, 700, 800, and 900 min). The WR of the sample was calculated[28] according to eq. (2):

$$\mathrm{WR}(\%) = \frac{m_2}{m_1} \times 100 \quad (2)$$

Characterization

Elemental analysis of WNMS, PAA, and WNMS–PAA was performed with a Vario EL cube (Elementar, Germany). An FTIR spectrometer (Shimadzu, 1.50SU1, Japan) was used to identify the vibrations in the functional groups presented in the samples. The spectra were obtained with 20 scans per sample

Table I. Effects of Different Parameters on the Water Absorbency of WNMS–PAA in Distilled Water and Salt Solutions

Effect	MBA (wt %)	APS (wt %)	BDK (wt %)	Neutralization degree of AA (%)	WNMS (wt %)	Reaction time (min)	Q_e (g/g)[a]	Q_e (g/g)[b]
Crosslinker	0.03	0.30	0.30	70	30	20	1203	32
	0.06	0.30	0.30	70	30	20	1268	93
	0.09	0.30	0.30	70	30	20	1366	159
	0.12	0.30	0.30	70	30	20	1663	161
	0.15	0.30	0.30	70	30	20	1456	101
	0.18	0.30	0.30	70	30	20	1141	39
Water-soluble initiator	0.12	0.00	0.30	70	30	20	703	31
	0.12	0.10	0.30	70	30	20	1206	39
	0.12	0.20	0.30	70	30	20	1401	48
	0.12	0.30	0.30	70	30	20	1663	161
	0.12	0.40	0.30	70	30	20	1680	196
	0.12	0.50	0.30	70	30	20	1176	33
Photoinitiator (BDK)	0.12	0.40	0.05	70	30	20	42	22
	0.12	0.40	0.10	70	30	20	623	119
	0.12	0.40	0.15	70	30	20	764	202
	0.12	0.40	0.20	70	30	20	793	220
	0.12	0.40	0.25	70	30	20	1698	228
	0.12	0.40	0.30	70	30	20	1680	196
Neutralization degree of AA (%)	0.12	0.40	0.25	65	30	20	135	92
	0.12	0.40	0.25	70	30	20	1698	228
	0.12	0.40	0.25	75	30	20	1073	231
	0.12	0.40	0.25	80	30	20	1292	240
	0.12	0.40	0.25	85	30	20	1701	388
	0.12	0.40	0.25	90	30	20	236	181
WNMS	0.12	0.40	0.25	85	0	20	998	100
	0.12	0.40	0.25	85	15	20	1406	140
	0.12	0.40	0.25	85	30	20	1701	388
	0.12	0.40	0.25	85	45	20	1033	173
	0.12	0.40	0.25	85	60	20	624	63
	0.12	0.40	0.25	85	75	20	368	36
Reaction time	0.12	0.40	0.25	85	30	5	1332	41
	0.12	0.40	0.25	85	30	10	1343	128
	0.12	0.40	0.25	85	30	15	1410	306
	0.12	0.40	0.25	85	30	20	1701	388
	0.12	0.40	0.25	85	30	25	1516	308
	0.12	0.40	0.25	85	30	30	1389	200

[a] Water absorbency of WMS-PAA in distilled water.
[b] Water absorbency of WMS-PAA in a 0.9 wt % NaCl solution.

ranging from 4000 to 400 cm^{-1}. The morphologies of the samples were analyzed by SEM (Shimadzu SSX-550, Japan). Before testing, the samples were sputter-coated with gold with an ETD-2000 auto sputter coater (Elaborate Technology Development Co., Ltd., China) with a current of 4 mA for 2 min. Thermogravimetric analysis (TGA) was performed on a thermogravimetric-differential thermal analysis (TG-DTA) instrument (Beijing Hengjiu Instrument, Ltd., Beijing, China) from 25 to 900°C at a heating rate of 10°C/min under a flowing air atmosphere. A Techcomp CT14D centrifuge (Shanghai, China) was used to calculate WR.

RESULTS AND DISCUSSION

Characterization of the Materials

Structure. ***Elemental analysis.*** As shown in Table II, the C content in WNMS–PAA increased from 34.24 to 35.66%, and the

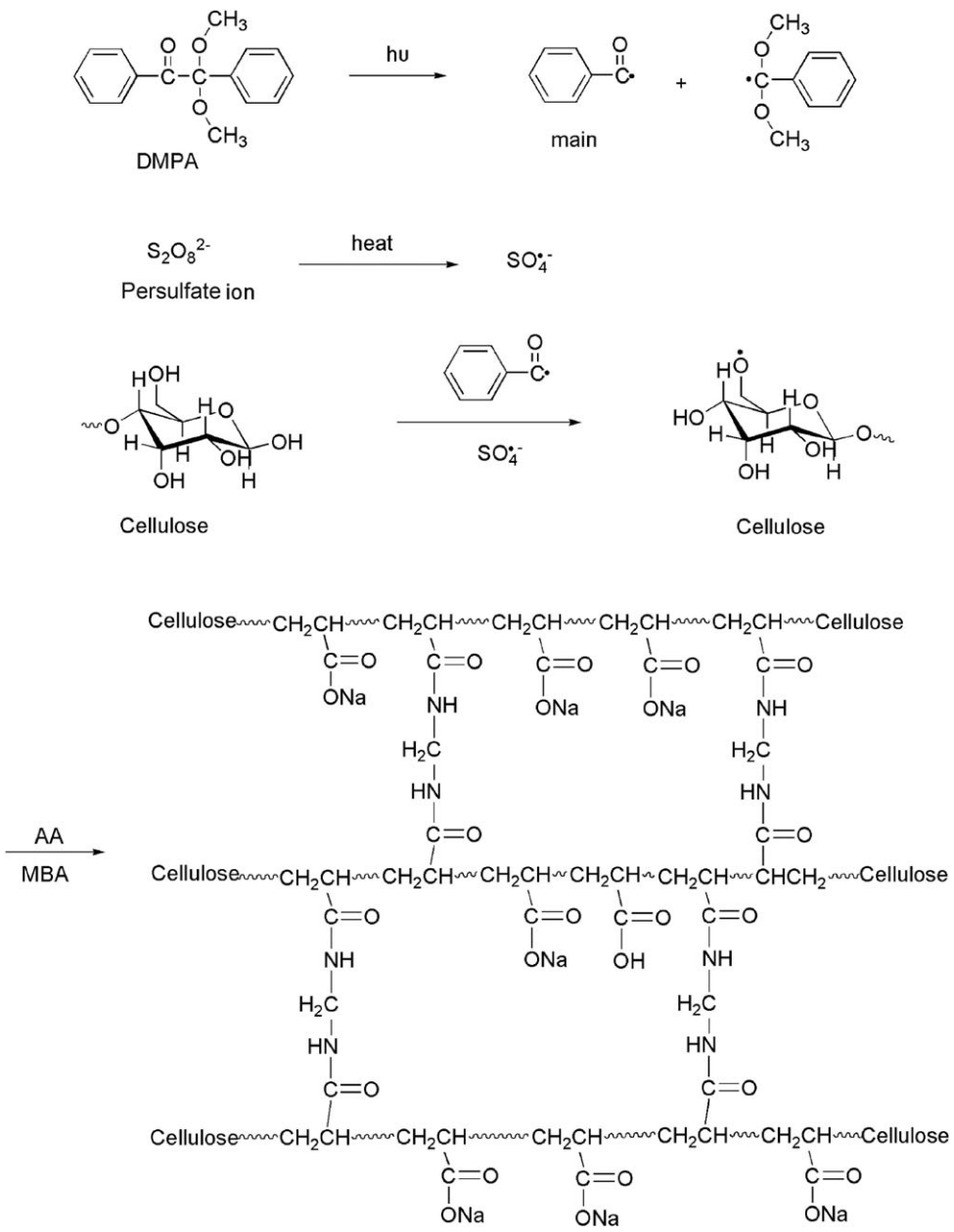

Figure 1. Proposed mechanism for the synthesis of WNMS–PAA. DMPA = dimethoxy-2-phenylacetophenone.

N content increased from 0.18 to 0.45% compared with PAA, whereas the H content decreased from 5.330 to 4.845%. This was because the cellulose molecules with relatively high carbon contents in WNMS reacted with the monomer molecules and changed the polymer chains. Meanwhile, part of the nitrogen-containing compound in WNMS was added to polymer chains; this led to increases in the C and N contents. The previous two reasons resulted in a slight decrease in the relative H content in WNMS–PAA.

FITR spectroscopy. The FTIR spectra of WNMS, PAA, and WNMS–PAA are shown in Figure 2. The spectrum of WNMS showed characteristic absorptions of cellulose structures, including the absorption at 3437 cm^{-1} (hydrogen bonded —OH stretching vibrations), 2939 cm^{-1} (methylene stretching), 1404 cm^{-1} (carbonyl stretching), and 1037 cm^{-1} (1,4-glycosidic bond). In the spectrum of PAA, the band at 3450 cm^{-1} was related to O—H and N—H stretching vibrations. The band at 2939 cm^{-1} resulted from the methylene stretching and O—H stretching of carboxylic acid. The absorption at 1680 cm^{-1} corresponded to the stretching of amide I. The band at 1562 cm^{-1} was due to the C=O asymmetric stretching of —COO— and amide II.[29] The two bands at 1404 and 1315 cm^{-1} contributed to the C=O symmetric stretching of the —COO—, stretching and bending vibrations of the C—N. Compared with PAA, the absorption peaks of WNMS–PAA revealed some changes in the characteristic spectral peaks. The peak at 2931 cm^{-1} (—COOH) was lower, and the ones at 1639 cm^{-1} (C=O of amide I), 1562

Table II. Elemental Analyses of WNMS, PAA, and WNMS–PAA

Sample	C (%)	N (%)	H (%)
WNMS	35.93	1.36	5.096
PAA	34.24	0.18	5.330
WNMS-PAA	35.66	0.45	4.845

cm^{-1}(COO— and amide II), and 1440 cm^{-1}(—COO—) were sharper in the spectrum of WNMS–PAA than in those of PAA. This indicates that these functional groups in WNMS grafted onto WNMS–PAA during the polymerization and —COOH groups transformed into —COO— groups during the neutralization of AA and WNMS.[30]

Morphology. The SEM micrographs of WNMS, PAA, and WNMS–PAA are depicted in Figure 3. We observed that WNMS showed a lamellar structure surface, and PAA showed a smooth, dense, and porous surface, whereas WNMS–PAA exhibited a comparatively coarse, loose, and porous surface. We concluded that the cellulose particles were added to polymer chains and many irregular aggregates were formed during the copolymerization reaction.[30] The coarse and improved surface of WNMS–PAA made the specific surface area of the superabsorbent materials increased; this was beneficial for the promotion of the water absorbency.

Thermal Properties. The thermal behavior of WNMS–PAA is shown in Figure 4. From the TG curve, we found that WNMS–PAA had a three-step thermogram, with weight losses of 28.97, 39.80, and 20.93%, respectively. The first stage occurring before 360°C was due to the water evaporation and the breaking of C—O—C bonds in the chain of WNMS. To be more exact, part of the CO_2 molecule eliminated from the polymeric backbone.[31] The major weight loss of the polymer occurred in the second stage between 360 and 538°C; this was assigned to the elimination of the water molecule from the two neighboring carboxylic groups of the polymer chains with the formation of anhydride, main-chain decomposition of the PAA, and destruction of crosslinked network structure.[32] The third stage occurred between 700 and 800°C; this might have been acceptable evidence for the further decomposition or degradation of residual organic matter at high temperatures. Ultimately, the weight of the residual sample was 10.30%; this was attributed to inorganic salts in the material and part of the decomposition of the product. Correspondingly, there were three peaks in the derivative TG curve at about 299, 426, and 744°C; this represented the maximum decomposition speeds.

Effects of the Different Parameters on the Water Absorbency of WNMS–PAA. The effect of different parameters on the distilled water and salt solution absorbency of WNMS–PAA are shown in Table I.

Effect of the crosslinker content on the water absorbency of WNMS–PAA. As shown in Table I, the water absorbency increased with the augment of crosslinker content from 0.03 to 0.12 wt % and then decreased with further increases in the crosslinker content. For an MBA to AA ratio of 0.12 wt %, the superabsorbent composite exhibited maximum absorbencies of 1663 g/g in distilled water and 161 g/g in a 0.9 wt % NaCl solution. For an MBA to AA ratio of less than 0.12 wt %, the increasing crosslinker raised the number of network nodes and improved the crosslinking density. This led to the formation of more three-dimensional polymer networks with a small aperture. These effects were favorable for fluid absorption and retention.[33] However, when the crosslinker content was too large (>0.12 wt %), the crosslinking density was higher, the holes in three-dimensional networks became smaller, and the elasticity of the polymeric network of the superabsorbent decreased. Then, the proposed structure failed to expand upon fluid wetting; this caused a decreased ability in the absorbing water. In summary, the superabsorbent composite with a moderate level of crosslinking can absorb and retain large quantities of aqueous fluids.

Effect of the initiator content on the water absorbency of WNMS–PAA. Table I illustrates the effect of the water-soluble initiator (APS) and photoinitiator (BDK) on the water absorbency of the prepared samples. The water absorbency increased with the augmentation of the APS and BDK contents from 0.0 to 0.4% and from 0.05 to 0.25%, respectively, and then decreased with the increasing APS and BDK content. The maximum absorbency was obtained when the content of APS was 0.4 wt % and that of BDK was 0.25 wt %. The reason was related to the relationship between the average chain length and concentration of the initiator in the polymerization.[34] It was assumed that with increasing initiator content, more radical centers and crosslinking density occurred; this could have promote the full reaction between the cellulose molecules and AA molecules. As a result, an effective three-dimensional polymer network could be formed, which might have enhanced the water absorbency. However, too many radical centers decreased the chain length and the molecular weight of the prepared polymer, which would bring about a lower water absorbency.[35]

Effect of the neutralization degree of AA on the water absorbency of WNMS–PAA. As shown in Table I, the water absorbency was quite low at a neutralization degree of 65% and higher at a

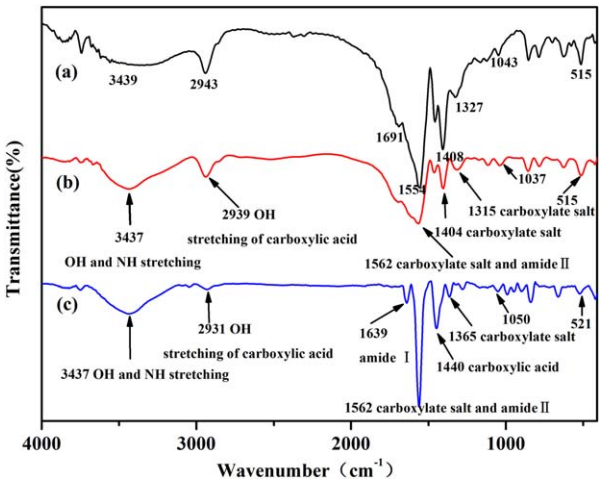

Figure 2. FTIR spectra of (a) WNMS, (b) PAA, and (c) WNMS–PAA. [Color figure can be viewed in the online issue, which is available at wileyonlinelibrary.com.]

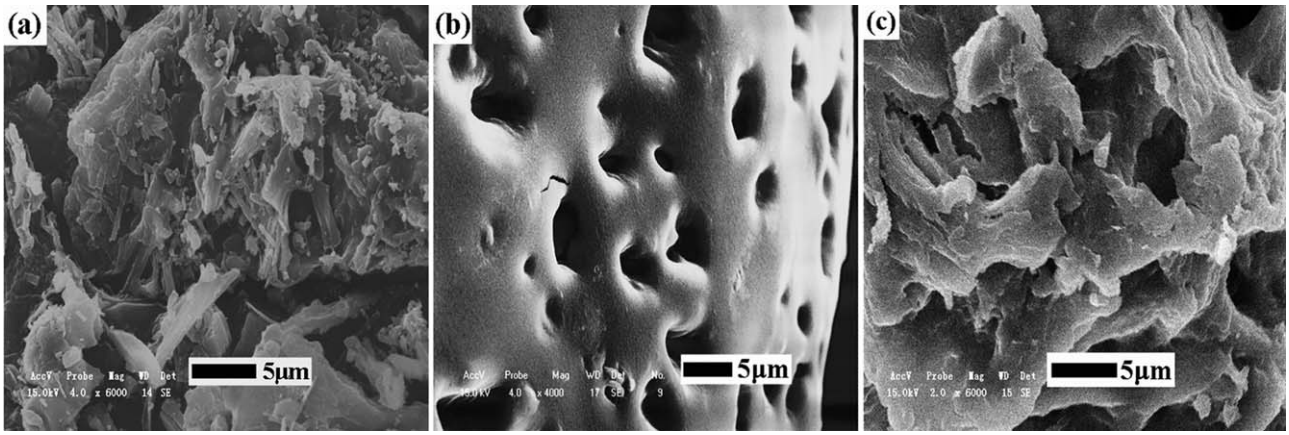

Figure 3. SEM micrographs of surfaces of (a) WNMS, (b) PAA, and (c) WNMS–PAA.

neutralization degree of 70%; this was caused by the increase in the ionic dissociation of the carboxylic acid groups.[36] The maximum absorbency (1701 g/g in distilled water and 388 g/g in 0.9 wt % NaCl solution) were obtained when the neutralization degree of AA was 85%. After AA was neutralized with a sodium hydroxide solution, the number of negatively charged carboxyl groups in the composite material and osmotic pressure increased and produced an electrostatic repulsion. Then, network expansion could be obtained. The electrostatic repulsion and osmotic pressure increased with the augmentation of the neutralization degree from 75 to 85%. This led to a high water absorbency. When the neutralization degree of AA exceeded 85%; however, the water absorbency of the prepared superabsorbent composite decreased. This behavior could have been due to a rise in the chain rubbery elasticity and counter-ion condensation on the polyion. We hold the opinion that the increasing numbers of Na^+ in the polymeric network led to the net charge density in the per unit chain length becoming higher; this may have contributed to the decline in the swelling ability.[18]

Effect of the WNMS content on the water absorbency of WNMS–PAA. The effect of the weight ratio of WNMS to AA on the water absorbency was studied, and the results are shown in Table I. The superabsorbent composites reached their maximum absorbency at a WNMS weight ratio of 30 wt % and then decreased. This effect was apparent for samples submersed either in distilled water or in saline solution. The maximum absorbency in distilled water was 1701 g/g, and that in a 0.9 wt % NaCl solution was 388 g/g. The absorbency in distilled water and that in a 0.9 wt % NaCl solution showed an increasing tendency in the ratio from 0 to 30 wt %; this was likely caused by increase in crosslinking between WNMS and PAA. WNMS contained a number of hydrophilic functional groups (—OH groups). Thus, reactions between the —OH groups of WNMS and the —COO— groups of AA occurred. Then, the polymeric network was enhanced, and this further caused a higher water absorbency.[37] The absorbencies in distilled water and the 0.9 wt % NaCl solution decreased at ratios over 30 wt %. This phenomenon may have been due to the conformation of more crosslinking points in the polymeric network; this would lead to an excessive increase in the crosslinking density of the superabsorbent hydrogel and a decrease in the water absorbency. Moreover, the phenomenon may have resulted in a relative ratio reduction in hydrophilic groups, such as —OH, —COOH, and —COO—, in the superabsorbent composite.

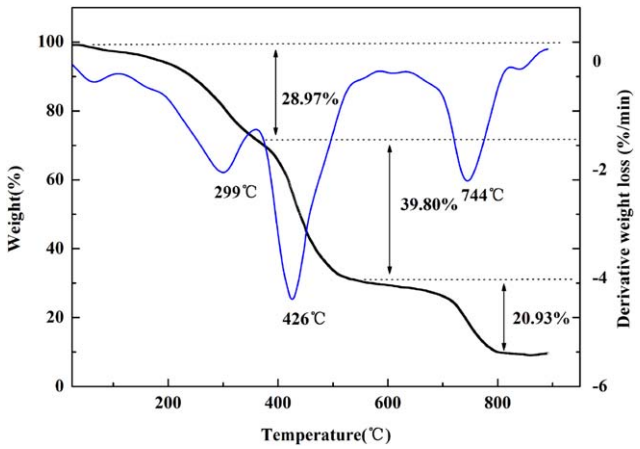

Figure 4. TGA thermogram of WNMS–PAA. [Color figure can be viewed in the online issue, which is available at wileyonlinelibrary.com.]

Effect of the reaction time on the water absorbency of WNMS–PAA. As shown in Table I, the water absorbency in distilled water and in the saline solution increased from 5 to 20 min and then decreased from 20 to 30 min. The maximum absorbency (1701 g/g in distilled water and 388 g/g in 0.9 wt % NaCl solution) was observed at 20 min. On one hand, a reaction time that was too short resulted in incomplete polymerization and a short polymer chain; this was not conducive to water absorption; On the other hand, an irradiation time that was too long resulted in an increase in polymer crosslinking degree; many branched chains were formed in the network structure, which tangled with each other and obstructed the expansion of the polymer. So, it produced small holes in three-dimensional networks, which led to the compounds absorbing little water.[35] Both of these respects resulted in a low water absorbency.

Water Retention

To evaluate the WR properties, high-temperature (60°C) drying and centrifugal separation methods (6000 rpm) was used

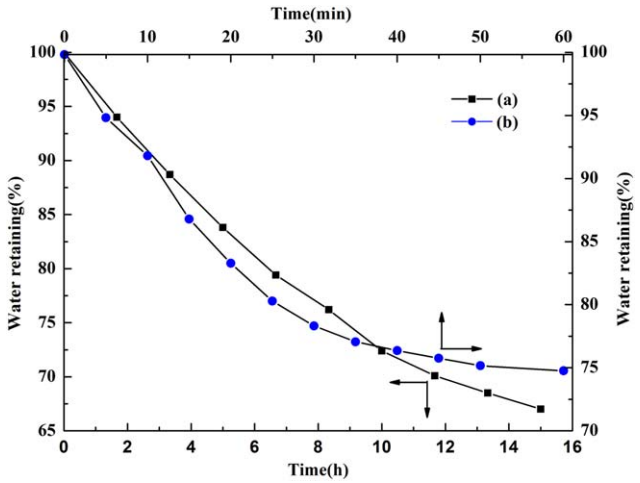

Figure 5. WR capacity of PAA–WNMS (a) dried at 60°C and (b) centrifuged at 6000 rpm. [Color figure can be viewed in the online issue, which is available at wileyonlinelibrary.com.]

to test the WR capacity. The results obtained by drying under a temperature of 60°C in an air oven are shown in Figure 5(a), and those obtained by centrifugation at speed of 6000 rpm under room temperature are shown in Figure 5(b). As shown in the figure, the WR maintained 68 and 75% WR after 15 h of drying and 60 min of centrifugation, respectively. The WR capacity could be determined by van der Waal's forces and the hydrogen-bonding interaction between the superabsorbent and water molecules.[38] The substantial carboxylate groups of WNMS–PAA made this chemical interaction stronger, and this improved the WR capacity.[1] The water loss ratio was larger in the first several hours than in the last several hours. The reason for this phenomenon was that at beginning, there was more weak-absorption water (easier to lose) on the polymer. As the extension of the drying and centrifugation time, the weak-absorption water was lower and lower, and the ratio of strong-absorption water was relatively larger in the hydrogel, and this led to a reduction in dehydration.

Swelling Kinetics

Swelling Behavior in Distilled Water and in a 0.9 wt % NaCl Solution. Figure 6(A,B) shows the effect of the contact time on the water absorbency in distilled water and in a 0.9 wt % NaCl solution, respectively. To investigate the kinetic mechanism, the pseudo-first-order and pseudo-second-order models were adopted to fit the experimental data.

The pseudo-first-order swelling kinetic model[39] is as follows:

$$\ln(Q_e - Q_t) = \ln Q_e - K_1 t \tag{3}$$

The pseudo-second-order swelling kinetic model[40,41] is as follows:

$$\frac{t}{Q_t} = \frac{1}{K_2 Q_e^2} + \frac{t}{Q_e} \tag{4}$$

where Q_e (g/g) and Q_t (g/g) are the water absorbencies at equilibrium and at time t (min), respectively, and K_1 (min^{-1}) and K_2 (g/g/min) are the rate constants.

As shown in Figure 6(A), the process of water absorption consisted of three steps: (1) an initial rapid increase phase at 0–60 min, where the absorption was fast and contributed significantly

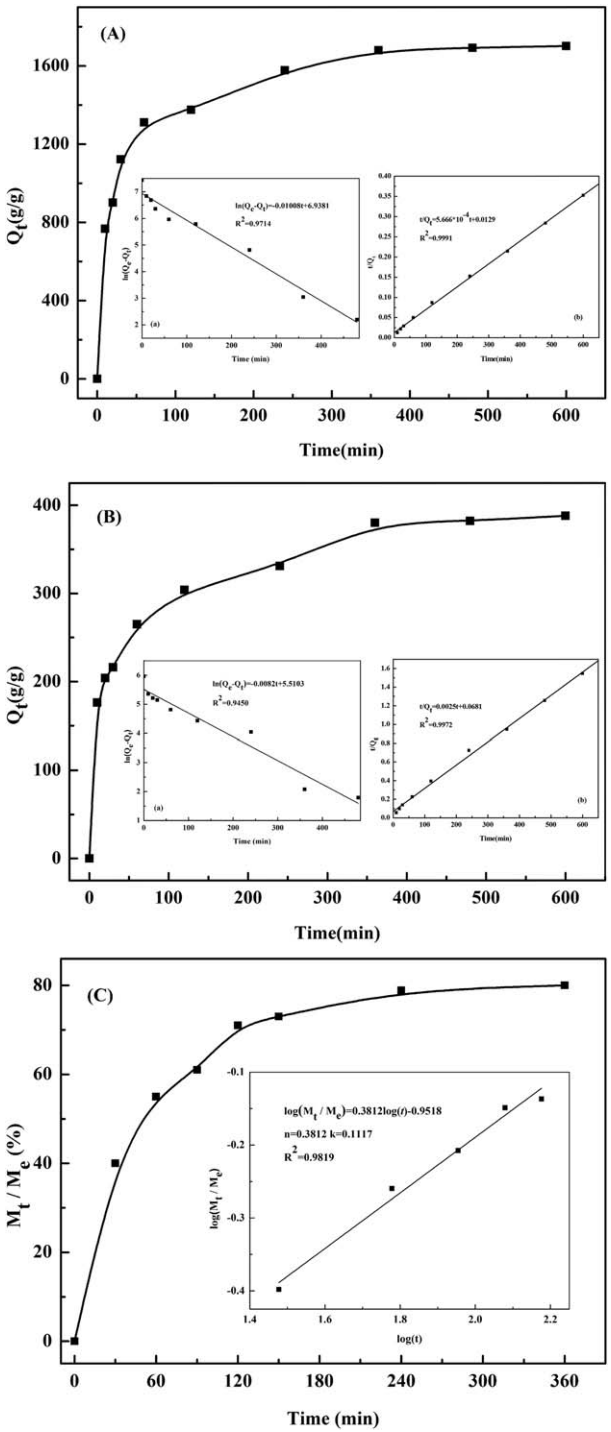

Figure 6. (A) Effect of the contact time on the distilled water absorbency: (a) pseudo-first-order kinetic model and (b) pseudo-second-order kinetic model. (B) Effect of the contact time on the salt solution absorbency (0.9 wt % NaCl): (a) pseudo-first-order kinetic model and (b) pseudo-second-order kinetic model. (C) Effect of the contact time on urea diffusion. The inset shows linear plots of the logarithm of diffusion fractions of urea against the log time in a 0.1 wt % urea solution.

Table III. Kinetic Parameters for the Water Absorbency of WMS–PAA in Distilled Water and 0.9 wt % NaCl Solutions

		Pseudo-first-order swelling kinetics			Pseudo-second-order swelling kinetics		
	$Q_{e,exp}$ (g/g)	K_1 (min^{-1})	$Q_{e,cal}$ (g/g)	R^2	K_2 (10^{-5} g/g/min)	$Q_{e,cal}$ (g/g)	R^2
Distilled water	1701	0.0101	1031	0.9714	2.4886	1765	0.9991
0.9 wt % NaCl solution	388	0.0082	247	0.9450	9.1777	400	0.9972

to the equilibrium uptake (>77%); (2) a slower second increase phase at 60–360 min, whose contribution to equilibrium absorption was relatively small (<23%); and (3) an equilibrium phase after 360 min, where absorption almost remained constant.

As shown in Figure 6(A), the pseudo-first-order plot (in part a) was linear with a linear correlation coefficient (R^2) of 0.9714 (Table III), and the value of the experimental absorption capacity ($Q_{e,exp}$) was 1701 g/g; this was much higher than the calculated value of the absorption capacity ($Q_{e,cal}$; 1031 g/g). The pseudo-second-order plot (in part b) also gave perfect straight lines with $R^2 = 0.9991$. $Q_{e,cal}$ (1765 g/g) was slightly higher than $Q_{e,exp}$ (1701 g/g). Therefore, this indicated that the swelling process in distilled water followed the pseudo-second-order swelling kinetic model.

As shown in Figure 6(B), the curve of water absorption in the 0.9 wt % NaCl solution also consisted of three phases:

1. An initial rapid increase phase at 0–60 min, in which the salt solution absorption rate was fastest and up to 69% of equilibrium absorption capacity.
2. A slower second increase phase in 60–360 min, whose contribution to equilibrium absorption was approximately 29%.
3. An equilibrium phase after 360 min, where absorption remained almost constant.

The dynamic swelling studies were done to characterize the mechanism of the 0.9 wt % NaCl solution absorption by the superabsorbent polymer via eqs. (3) and (4). As shown in Figure 6(B), the pseudo-first-order plot (in part a) and the pseudo-second-order plot (in part b) were linear with R^2 values of 0.9450 and 0.9972, and the $Q_{e,cal}$ values were 247 and 400 g/g, respectively. They were 36 and 3.1% differences in the value of the salt solution $Q_{e,exp}$ (388 g/g). Therefore, this indicated that the swelling process in a 0.9 wt % NaCl solution followed the pseudo-second-order swelling kinetic model. The good agreement with pseudo-second-order swelling kinetic model explained that the absorption determining step may have been valence forces through the sharing or exchange of electrons between WNMS–PAA and the salt solution.[42]

Swelling Behavior in a Urea Solution. The water absorbency in the 0.1 wt % urea solution was measured three times by eq. (1), and the average value of equilibrium absorbency was 1011 g/g. The water absorption rate in urea solution was reduced to 59.5% relative to the equilibrium absorbency in distilled water (1701 g/g). This was because urea was a nonelectrolyte existing in the molecules and a nonionized form in aqueous solution.[18] The existence of urea caused osmotic pressure differentials in the superabsorbent polymer solutions, and this may have caused thewater molecules to move in the direction of the electrolyte dilution concentration. Thus, urea-based fertilizers reduced the water absorbency of the superabsorbent polymer.

As shown in Figure 6(C), the diffusion capacity of urea increased rapidly from 0 to 30 min, and more than 40% of the total amount of urea diffusion into the gels occurred within 30 min. The urea diffusion capacity decreased gently in the later 90 min, but there was still nearly 31% urea diffusion into the gels. After 120 min, the diffusion rate slowed down rapidly until it reached the maximum amount of diffusion close to 80% of the total amount of urea. This phenomenon was due to the existence of intermolecular forces between the urea molecules and polymer chains and the osmotic pressure of the urea solution. The osmosis of the solution and hydrogen-bonding interactions between the urea molecules and the groups of the polymer was strong at first, and this led to a relatively high absorbency. With a prolonged contact time, further interaction of the groups gradually weakened; this slowed down the speed of water absorption until it reached equilibrium absorbency.

The study on the urea diffusion mechanism is very important for practical hydrogel applications. To further understand the urea diffusion mechanism, the results were analyzed to estimate the values of n and k with an empirical equation[43] as follows:

$$\log(M_t/M_e) = \log(k) + n\log(t) \quad (5)$$

where M_e is the amount of urea at equilibrium, n is a diffusion exponent that indicates the diffusion mechanism, and k is a diffusion constant. A good linear fit with an R^2 of 0.9819 was observed between $\log(M_t/M_e)$ and $\log t$ for $M_t/M_e \leq 0.6$. From the slope and intercept of the plot of $\log(M_t/M_e)$ versus $\log t$, the kinetic parameters n and k were calculated, and the value were 0.3812 and 0.1117, respectively. According to the classification of the diffusion mechanism, a value of $n < 0.5$ indicated the Fickian diffusion mechanisms. The calculated value for the constant $n = 0.3812$, the urea diffusion mechanism of the hydrogels was a Fickian diffusion mechanism.

CONCLUSIONS

A novel superabsorbent hydrogel (WNMS–PAA) was synthesized by the UV irradiation method in the presence of BDK and APS as initiators and MBA as a crosslinker. The structure and properties of WNMS–PAA were analyzed by FTIR spectroscopy, SEM, and TGA, the consequences of which indicated the occurrence of the copolymerization process. A condition experiment was conducted on the neutralization degree of AA, reaction time, and amounts of AA, WNMS, MBA, APS, and BDK. The optimal conditions were m(AA)/m(WNMS)/m(MBA)/

m(APS)/*m*(BDK) = 100:30:0.12:0.40:0.25 (where *m* is the abbreviation of mass), neutralization degree of AA = 85%, and reaction time = 20 min. The water absorbencies of the WNMS–PAA in distilled water, 0.9 wt % in NaCl solution and 0.1 wt % in urea solution were 1701, 388, and 1011 g/g, respectively. The swelling process in distilled water and in 0.9 wt % NaCl solution followed the pseudo-second-order swelling kinetic model. Moreover, almost 80% of the total amount of urea in the 0.1 wt % urea solution diffused into the hydrogel, and the diffusion process was consistent with a Fickian diffusion mechanism. In addition, our synthesized superabsorbent WNMS–PAA composite showed better properties of water swelling, WR, and urea absorption compared to the same type of superabsorbent materials.[1,18,25] Thus, it could be exploited very well in many potential applications, including agriculture, forestry horticulture, pharmaceuticals, and other industries. The application and degradation of the product will be explored in our future research work.

ACKNOWLEDGMENTS

The authors are grateful to the Resource Evaluation Sector of the China Geological Survey (contract grant number 1212011220797), the Basic Research Program of the Jilin Provincial Science and Technology Department (contract grant number 20130102040JC), and Changchun Science and Technology Plan Projects (contract grant number 13NK01) for their financial support.

REFERENCES

1. Zhou, Y.; Fu, S.; Zhang, L.; Zhan, H. *Carbohydr. Polym.* **2013**, *97*, 429.
2. Jin, S.; Wang, Y.; He, J.; Yang, Y.; Yu, X.; Yue, G. *J. Appl. Polym. Sci.* **2013**, *128*, 407.
3. Zhong, K.; Lin, Z.-T.; Zheng, X.-L.; Jiang, G.-B.; Fang, Y.-S.; Mao, X.-Y.; Liao, Z.-W. *Carbohydr. Polym.* **2013**, *92*, 1367.
4. Sadeghi, M.; Hosseinzadeh, H. *J. Bioact. Compat. Polym.* **2008**, *23*, 381.
5. Singh, A.; Sharma, P. K.; Garg, V. K.; Garg, G. *Int. J. Pharm. Sci. Rev. Res.* **2010**, *4*, 97.
6. Pourjavadi, A.; Farhadpour, B.; Seidi, F. *Starch* **2008**, *60*, 457.
7. Zheng, Y.; Wang, A. *Chem. Eng. J.* **2012**, *200*, 601.
8. Saxena, A. K. *J. Thorac. Cardiovasc. Surg.* **2010**, *139*, 496.
9. Yi, J.-Z.; Zhang, L.-M. *Bioresour. Technol.* **2008**, *99*, 2182.
10. Zou, W.; Yu, L.; Liu, X.; Chen, L.; Zhang, X.; Qiao, D.; Zhang, R. *Carbohydr. Polym.* **2012**, *87*, 1583.
11. Akar, E.; Altinisik, A.; Seki, Y. *Carbohydr. Polym.* **2012**, *90*, 1634.
12. Zhang, S.; Zhou, Y.; Nie, W.; Song, L. *Cellulose* **2012**, *19*, 2081.
13. Saber-Samandari, S.; Gazi, M.; Yilmaz, E. *Polym. Bull.* **2012**, *68*, 1623.
14. Li, Q.; Ma, Z.; Yue, Q.; Gao, B.; Li, W.; Xu, X. *Bioresour. Technol.* **2012**, *118*, 204.
15. Xie, L.; Liu, M.; Ni, B.; Wang, Y. *Ind. Eng. Chem. Res.* **2012**, *51*, 3855.
16. Zhang, J.; Wu, Y.; Zhang, Z.; Ao, C. *J. Inner Mongolia Agric. Sci. Technol.* **2000**, *6*, 14.
17. Chen, J. C.; Shen, H. S.; Tang, B. S.; Li, Y. B.; Pen, D. Q. *Chin. Agric. Sci. Bull.* **2006**, *122*, 410.
18. Cheng, Z.; Li, J.; Yan, J.; Kang, L.; Ru, X.; Liu, M. *J. Appl. Polym. Sci.* **2013**, *130*, 3674.
19. Sorour, M.; El-Sayed, M.; Abd El Moneem, N.; Talaat, H. A.; Shalaan, H.; El Marsafy, S. *Starch* **2013**, *65*, 172.
20. Ebrahimi, R. *Iran. Polym. J.* **2011**, *21*, 11.
21. Bardajee, G. R.; Hooshyar, Z.; Zehtabi, F.; Pourjavadi, A. *Iran. Polym. J.* **2012**, *21*, 829.
22. Lee, J. S.; Kumar, R.; Rozman, H.; Azemi, B. *Food Chem.* **2005**, *91*, 203.
23. Raafat, A. I.; Eid, M.; El-Arnaouty, M. B. *Nucl. Instrum. Methods Phys. Res. Sect. B* **2012**, *283*, 71.
24. Wan, T.; Huang, R.; Zhao, Q.; Xiong, L.; Luo, L.; Tan, X.; Cai, G. *J. Appl. Polym. Sci.* **2013**, *130*, 698.
25. Chiou, B.-S.; Jafri, H.; Cao, T.; Robertson, G. H.; Gregorski, K. S.; Imam, S. H.; Glenn, G. M.; Orts, W. J. *J. Appl. Polym. Sci.* **2013**, *129*, 3192.
26. Ahmed, E. M.; Aggor, F. S.; Awad, A. M.; El-Aref, A. T. *Carbohydr. Polym.* **2013**, *91*, 693.
27. Watt, G. W.; Chrisp, J. D. *Anal. Chem.* **1954**, *26*, 452.
28. Zhang, Y.; Wu, F.; Liu, L.; Yao, J. *Carbohydr. Polym.* **2013**, *91*, 277.
29. Wan, T.; Huang, R.; Zhao, Q.; Xiong, L.; Qin, L.; Tan, X.; Cai, G. *J. Appl. Polym. Sci.* **2013**, *130*, 3404.
30. Liu, J.; Li, Q.; Su, Y.; Yue, Q.; Gao, B.; Wang, R. *Carbohydr. Polym.* **2013**, *94*, 539.
31. Sand, A.; Yadav, M.; Behari, K. *Carbohydr. Polym.* **2010**, *81*, 97.
32. Bao, Y.; Ma, J.; Li, N. *Carbohydr. Polym.* **2011**, *84*, 76.
33. Li, Y.; Ren, N.; Wang, Y.; Huang, J.; Liu, W.; Su, Z.; Yang, J. *J. Appl. Polym. Sci.* **2013**, *130*, 2184.
34. Liu, Z.; Miao, Y.; Wang, Z.; Yin, G. *Carbohydr. Polym.* **2009**, *77*, 131.
35. Ma, Z.; Li, Q.; Yue, Q.; Gao, B.; Xu, X.; Zhong, Q. *Bioresour. Technol.* **2011**, *102*, 2853.
36. Kiani, A.; Asempour, H. *J. Appl. Polym. Sci.* **2012**, *126*, E477.
37. Liu, J.; Li, Q.; Su, Y.; Yue, Q.; Gao, B.; Wang, R. *Carbohydr. Polym.* **2013**, *94*, 539.
38. Patra, T.; Pal, A.; Dey, J. *Langmuir* **2010**, *26*, 7761.
39. Chiou, M. S.; Li, H. Y. *J. Hazard Mater.* **2002**, *93*, 233.
40. Ho, Y. S.; McKay, G. *Process Biochem.* **1999**, *34*, 451.
41. Schott, H. *J. Macromol. Sci. Phys.* **1992**, *31*, 1.
42. Liu, J.; Su, Y.; Li, Q.; Yue, Q.; Gao, B. *Bioresour. Technol.* **2013**, *143*, 32.
43. Peppas, N. A.; Gurny, R.; Doelker, E.; Buri, P. *J. Membr. Sci.* **1980**, *7*, 241.